AIP | Review of Scientific Instruments

Noise reduction in functional near-infrared spectroscopy signals by independent component analysis

Hendrik Santosa, Melissa Jiyoun Hong, Sung-Phil Kim, and Keum-Shik Hong

Citation: Review of Scientific Instruments **84**, 073106 (2013); doi: 10.1063/1.4812785
View online: http://dx.doi.org/10.1063/1.4812785
View Table of Contents: http://scitation.aip.org/content/aip/journal/rsi/84/7?ver=pdfcov
Published by the AIP Publishing

Noise reduction in functional near-infrared spectroscopy signals by independent component analysis

Hendrik Santosa,[1] Melissa Jiyoun Hong,[2] Sung-Phil Kim,[3] and Keum-Shik Hong[1,4,a)]
[1]*Department of Cogno-Mechatronics Engineering, Pusan National University, 30 Jangjeon-dong, Geumjeong-gu, Busan 609-735, South Korea*
[2]*Department of Education Policy and Social Analysis, Columbia University, 116th Street and Broadway, New York, New York 10027, USA*
[3]*Department of Brain and Cognitive Engineering, Korea University, Anam 5 ga, Seongbuk-gu, Seoul 136-713, South Korea*
[4]*School of Mechanical Engineering, Pusan National University, 30 Jangjeon-dong, Geumjeong-gu, Busan 609-735, South Korea*

(Received 3 May 2013; accepted 19 June 2013; published online 10 July 2013)

Functional near-infrared spectroscopy (fNIRS) is used to detect concentration changes of oxy-hemoglobin and deoxy-hemoglobin in the human brain. The main difficulty entailed in the analysis of fNIRS signals is the fact that the hemodynamic response to a specific neuronal activation is contaminated by physiological and instrument noises, motion artifacts, and other interferences. This paper proposes independent component analysis (ICA) as a means of identifying the original hemodynamic response in the presence of noises. The original hemodynamic response was reconstructed using the primary independent component (IC) and other, less-weighting-coefficient ICs. In order to generate experimental brain stimuli, arithmetic tasks were administered to eight volunteer subjects. The *t*-value of the reconstructed hemodynamic response was improved by using the ICs found in the measured data. The best *t*-value out of 16 low-pass-filtered signals was 37, and that of the reconstructed one was 51. Also, the average *t*-value of the eight subjects' reconstructed signals was 40, whereas that of all of their low-pass-filtered signals was only 20. Overall, the results showed the applicability of the ICA-based method to noise-contamination reduction in brain mapping. © *2013 AIP Publishing LLC*. [http://dx.doi.org/10.1063/1.4812785]

I. INTRODUCTION

The use of the independent component analysis (ICA) method[1] was investigated as a means of analyzing functional near-infrared spectroscopy (fNIRS) signals and removing noise.[2] ICA, which obtains independent components (ICs) from signals with unobservable sources, has been established in recent years as an effective technique for blind separation of independent sources.[3] The purpose of ICA can be explained the example of the classical "cocktail party" problem. In such a context, at any one moment, many people are talking amid a cacophony of background noises (e.g., music). If a microphone records a mixture of voices the mixing properties of which can be determined, the respective voice-signal origins can be independently identified. ICA has been utilized as a fundamental tool in many fields, though its most classical application is image-noise reduction.[4] Additionally, it has been employed by many researchers employing neuroimaging techniques fields including electroencephalography (EEG),[5,6] fNIRS,[7,8] and functional magnetic resonance imaging (fMRI).[9,10]

The fNIRS-measured hemodynamic response is contaminated by the noises of physiological processes[11–13] (i.e., low-frequency oscillations[14,15] as well as respiratory[16] and cardiac activities[17]), motion artifacts (e.g., from body/head movement[18]), optode movement, and instrument degradation (e.g., temporal differences in the baseline laser characteristics[19]). fNIRS data preprocessing usually involves filtering such noises in order to obtain higher-quality topographic images. But whereas some physiological noises (i.e., respiratory and cardiac activities) can be removed using a low-pass filter (LPF),[20] low-frequency (e.g., 0.15 Hz) oscillatory noises and motion artifacts cannot. Alternatively, unwanted noises and artifacts from fNIRS signals can be removed using linear regression,[21] least mean squares adaptive filtering,[22] and ICA.[23–26]

Continuous-wave-type fNIRS measures the optical intensity changes[27] at two wavelengths,[28] which results are then converted to hemodynamic concentration changes using the modified Beer-Lambert law. In recent years, fNIRS has emerged as a promising non-invasive technique for near-infrared-light-range (650–950 nm) monitoring of changes in the cerebral hemodynamic response.[29–33] The advantages of fNIRS compared with fMRI[34] or positron emission tomography[35,36] include higher temporal resolution, improved safety, portability, and lower cost. In order to extend and enhance the applicability of fNIRS, the noise-reduction capabilities of fNIRS-based brain-computer interface system is a current research issue that needs to be addressed.

The present study administered simple arithmetic (addition and subtraction) tasks to volunteer subjects and investigated the hemodynamic changes in the prefrontal cortex in developing the ICA-based noise-reduction scheme herein

a)Author to whom correspondence should be addressed. Electronic mail: kshong@pusan.ac.kr.

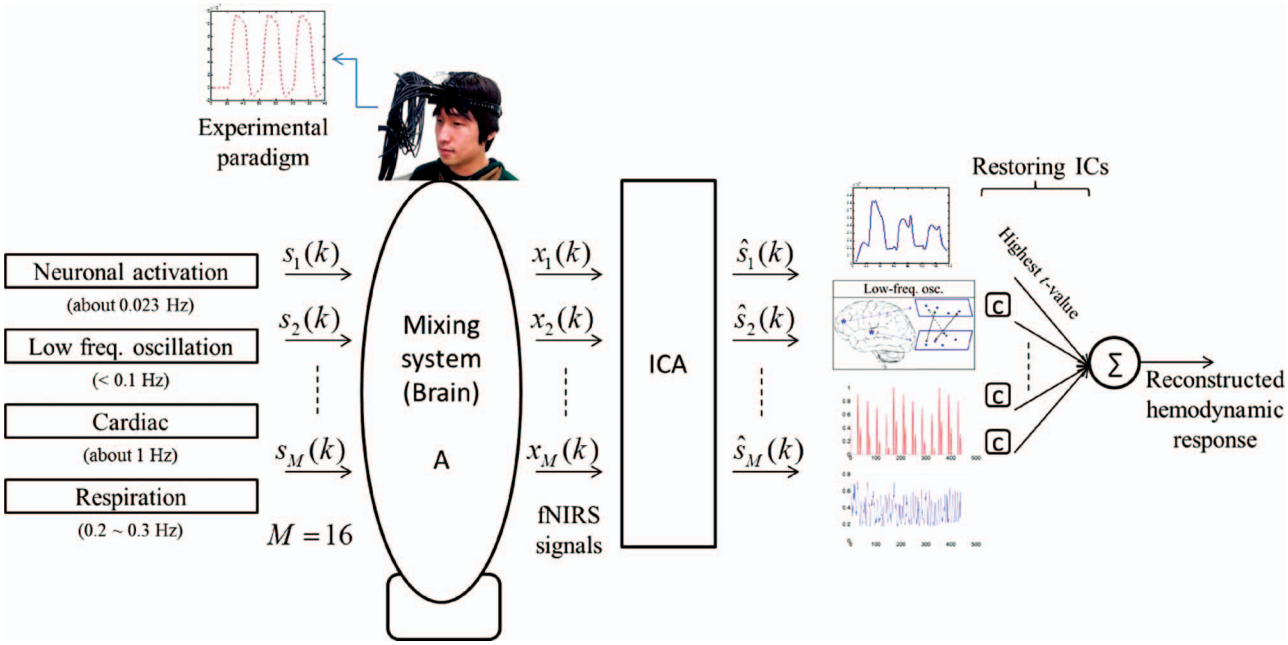

FIG. 1. The proposed ICA method: The original hemodynamic response is reconstructed using independent components (ICs).

proposed. Several studies over the past decade have applied fMRI and arithmetic tasks to the study of brain activity.[37] A number of studies also have used fNIRS to examine the prefrontal cortex[38,39] and the left and right hemispheres.[40] With the ICA method, detection of arithmetic-task-stimulated neuronal activities, in which oxygenation changes in the hemodynamic responses are more vivid than in the resting state, is enhanced. Specifically, the proposed method, compared with low-pass-filtering, significantly improves the signal-to-noise ratio (SNR), thereby enabling clearer image reconstruction.

II. MATERIALS AND METHODS

A. ICA theory

A schematization of the proposed ICA method is provided in Figure 1. Let $x_i(k)$, $i = 1, 2, \ldots, M$, denote the measured fNIRS data, where M is the total number of channels, subscript i is the ith channel, k (= 1, 2, …, N) is the discrete time, and N is the number of samples (in this study, $M = 16$ and $N = 796$).

Further, let $s_i(k)$, $i = 1, 2, \ldots, M$, be the unknown source signals. Then, the measured fNIRS signals can be written as

$$\mathbf{x}(k) = A\,\mathbf{s}(k), \quad k = 1, 2, \ldots, N, \tag{1}$$

where $\mathbf{x}(k) = [x_1(k)\ \ x_2(k)\ \ \cdots\ \ x_M(k)]^{\mathrm{T}}$, $\mathbf{s}(k) = [s_1(k)\ \ s_2(k)\ \ \ldots\ \ s_M(k)]^{\mathrm{T}}$, and $A \in R^{M\times M}$ is an unknown constant matrix (i.e., a mixing matrix) representing the weighting coefficients of the respective ICs' influence on the measured signals, and $\mathbf{x}(k) \in R^{M\times 1}$ and $\mathbf{s}(k) \in R^{M\times 1}$ are the column vectors representing the measured hemodynamic responses and the ICs, respectively, at each time point. Given $\mathbf{x}(k)$, the issue now is how both A and $\mathbf{s}(k)$ are to be estimated. The ICs' $\hat{s}_i(k)$ are written as

$$\hat{s}_i(k) = \mathbf{w}_i^T\mathbf{x}(k), \quad k = 1, 2, \ldots, N, \tag{2}$$

where $\mathbf{w}_i$ is a column vector to be determined.

The basic purpose of ICA is to consider the non-Gaussianity of measured signals and to find their projections. ICA estimates $\mathbf{w}_i$ by maximizing the non-Gaussianity of $\mathbf{w}_i{}^{\mathrm{T}}\mathbf{x}(k)$ upon the observed data $\mathbf{x}(k)$. If the projections afford consistent IC estimates, it can be concluded that $\mathbf{w}_i$ was well chosen. ICA estimation entails two steps: preliminary whitening of data, and estimation of an orthogonal ICA transform.[1] It has been noted that performing ICA decomposition several times yields similar ICs.[41]

After estimating each $\mathbf{w}_i$, the ICs are estimated using the equation

$$\hat{\mathbf{s}}(k) = W\,\mathbf{x}(k), \quad k = 1, 2, \ldots, N, \tag{3}$$

where $W = [\mathbf{w}_1\ \mathbf{w}_2\ \cdots\ \mathbf{w}_M]^{\mathrm{T}}$. ICA's potent blind-separation utility makes possible the separation of various noises within fNIRS data, resulting in an enhanced stimuli-prompted hemodynamic response.

B. ICA concept

Figure 2 illustrates the ICA concept. Let the five signals in Figure 2(a) (i.e., h_1, h_2, h_3, h_4, and h_5) represent hemodynamic signals and the power-spectral densities (PSDs) of which are depicted in Figure 2(b). Let the signals in Figure 2(c) be mixed signals from Figure 2(a) (i.e., $1.0h_1 + 0.9h_2 + 1.1h_3 + 0.3h_4 + 0.7h_5$, $0.5h_1 + 1.3h_2 + 1.2h_3 + 0.5h_4 + 0.5h_5$, $0.7h_1 + 1.4h_2 + 0.9h_3 + 0.1h_4 + 0.9h_5$, $0.5h_1 + 0.5h_2 + 0.5h_3 + 0.7h_4 + 0.8h_5$, $0.2h_1 + 1.5h_2 + 1.3h_3 + 0.9h_4 + 0.1h_5$, etc.). Now, it is assumed that only three of the five signals in Figure 2(c) are measured (i.e., the measurement is insufficient) and that the ICA method is applied only to those three signals, resulting in Figure 2(d). In comparing Figures 2(a) and 2(d)

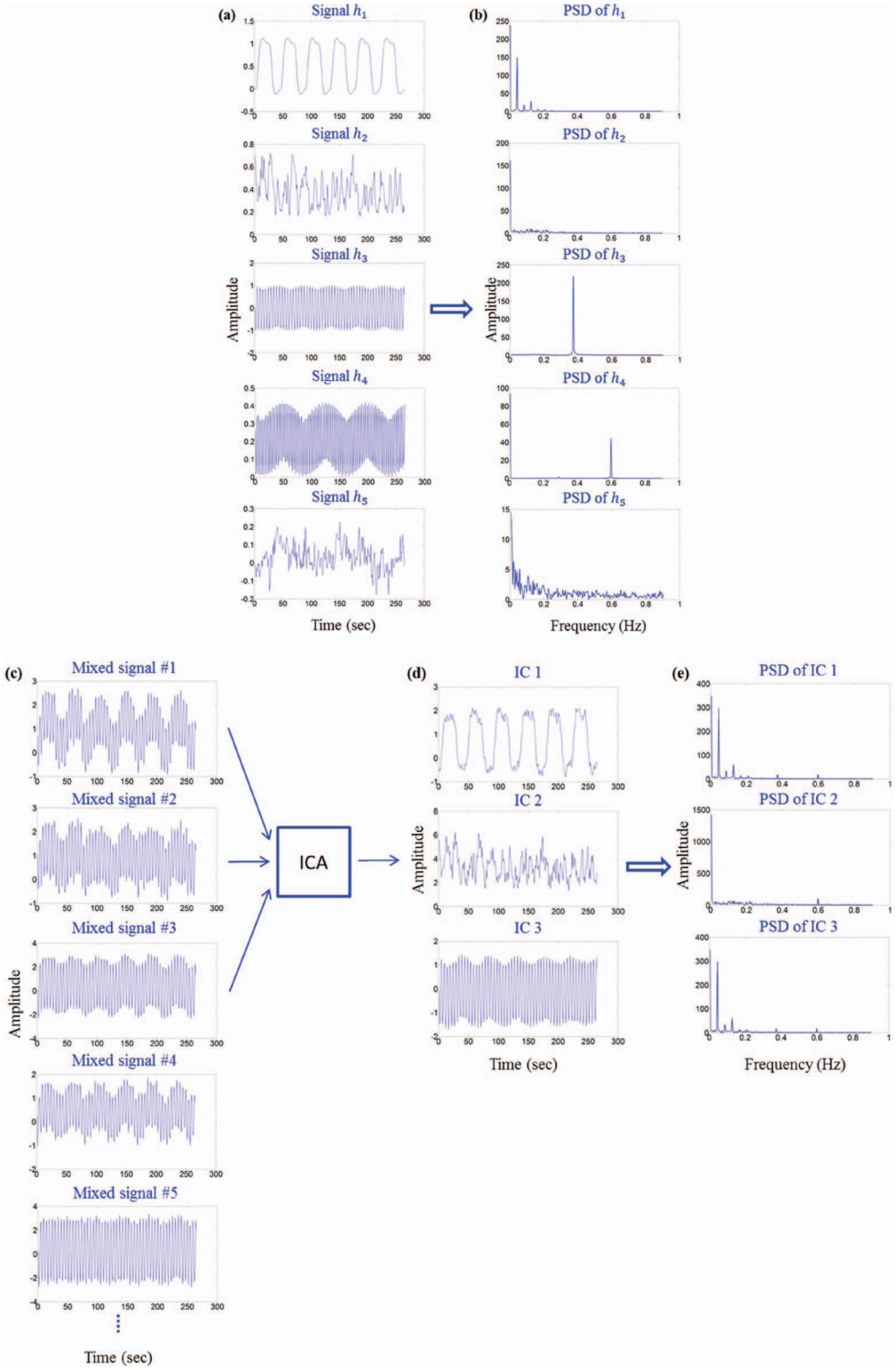

FIG. 2. ICA concept: (a) examples of 5 hemodynamic signals (i.e., a hemodynamic response due to neuronal activation, low frequency oscillation #1, respiratory, motion artifact, and low frequency oscillation #2), (b) the power-spectral densities of (a), (c) three signals used in the ICA of http://www.cis.hut.fi/projects/ica/fastica, (d) three identified ICs from (c), and (e) the power-spectral densities of (d) that can be compared with (b), where IC 1, IC 2, and IC 3 are claimed to be the estimated hemodynamic responses $\hat{h}_1$, $\hat{h}_2$, and $\hat{h}_3$, respectively.

and their power-spectral densities in Figures 2(b) and 2(e), respectively, it can be seen that the ICA method effectively retrieved the original source signals from the noisy mixed signals shown in Figure 2(c). This strategy is particularly useful for replicating the variation of measured signals. When using ICA, the IC associated with the applied stimuli might not be the dominant one, or there might exist multiple such ICs. But by referencing the spectrums of the identified ICs, we can determine the particular hemodynamic signal having the same density (Figure 2(b)).

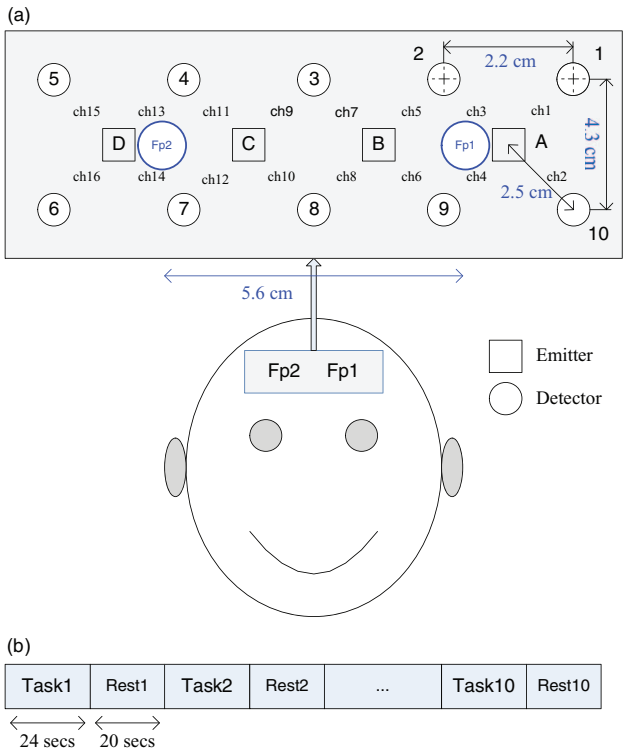

FIG. 3. Experimental design: (a) optodes configuration (Fp1 and Fp2 in the International 10-20 System are used as reference points), (b) experimental procedure for arithmetic task.

C. Subjects

Eight students participated in the experiment (all males, aged 28 ± 5 years, none having a history of any neurological disorder). All of the subjects had provided written consent. The experiment was conducted in accordance with the ethical standards outlined in the latest Declaration of Helsinki. It entailed having each of the subjects sit on a chair and solve arithmetic problems provided to him on a piece of paper.

D. Data acquisition

The experimental data were acquired from a NIRS imaging system (DYNOT: DYnamic Near-infrared Optical Tomography; NIRx Medical Technologies, Brooklyn, NY) at a sampling rate of 1.81 Hz. The data were measured simultaneously at two wavelengths (760 nm and 830 nm) using 14 optodes. As Figure 3(a) indicates, Fp1 and Fp2, in the International 10-20 System, were utilized as reference points (distance between Fp1 and Fp2: 5.6 cm).

The diagonal distance between an emitter and a detector is 2.5 cm, the vertical distance between two detectors 4.3 cm, the horizontal distance between them 2.2 cm, and the distance between two sources 2.2 cm. The oxy-hemoglobin (HbO) and deoxy-hemoglobin (HbR) concentration-level changes were computed using the modified Beer-Lambert law

$$\Delta\phi_i(\lambda, t) = -\ln\frac{U_i(\lambda, t)}{U_i^o(\lambda, t)} = [a^{HbO}(\lambda)\Delta c_i^{HbO}(t) + a^{HbR}(\lambda)\Delta c_i^{HbR}(t)]\, d_i l_i, \quad (4)$$

where i is the channel index, λ is the wavelength of the laser source, $\Delta\phi(\lambda, t)$ is the optical density variation at time t, $U^o(\lambda, t)$ and $U(\lambda, t)$ are the photon fluxes at the source and detector positions, respectively, a^{HbO} and a^{HbR} are the absorption coefficients of HbO and HbR, respectively, Δc_i^{HbO} and Δc_i^{HbR} are the concentration changes of HbO and HbR, respectively, d_i is the differential path length factor (in this study, constant values for all channels, $d_i = 7.15$ for $\lambda = 760$ nm and $d_i = 5.98$ for $\lambda = 830$ nm that are the default values in the NAVI software, were used), and l is the distance between the source and the detector. A total of 16 channels were used, including four sources and 10 detectors, as shown in Figure 3(a).

E. Stimuli

Throughout the experimental session, each subject performed two types of randomly appearing two-digit arithmetic tasks (addition and subtraction of integers; e.g., 15 + 12, 23 − 6). The session consisted of a 24-s task period followed by a 20-s rest period, and was repeated 10 times (Figure 3(b)). Accordingly, the total experimental duration was 440 s.

F. ICA processing

To help illustrate the performance of the proposed ICA method, two other hemodynamic signals were generated: a modeled (or desired) hemodynamic response and low-pass filtering of the fNIRS signal (Figure 4). The modeled hemodynamic response, denoted $h_M(k)$ in Figure 4, represents the expected hemodynamic response to the given stimuli,

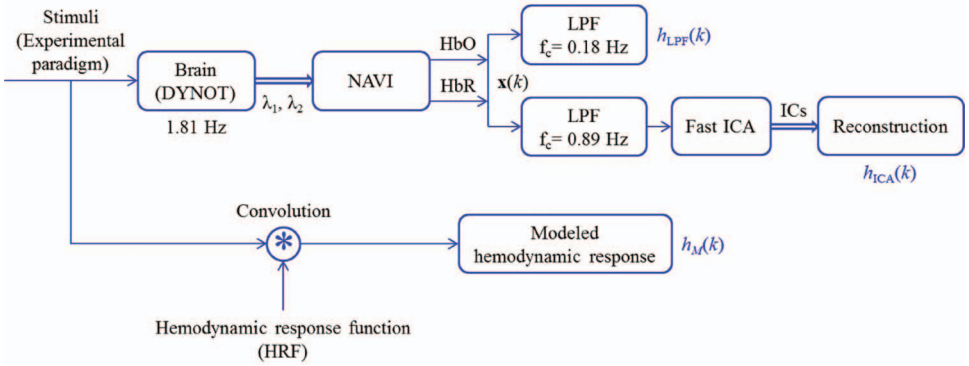

FIG. 4. Processing scheme.

computed by convolving the stimuli pattern in Figure 3(b) and a typical hemodynamic response function as

$$h_M(k) = \sum_{n=-\infty}^{\infty} Box(n)\, h(k-n), \tag{5}$$

where $Box(k)$ is the box-type stimuli pattern and $h(k)$ is the hemodynamic response function adopted from the SPM8 (Wellcome Trust Centre for Neuroimaging, London, UK).[42]

To obtain the HbO and HbR concentration changes from the DYNOT signals, NAVI open-source software (Near-

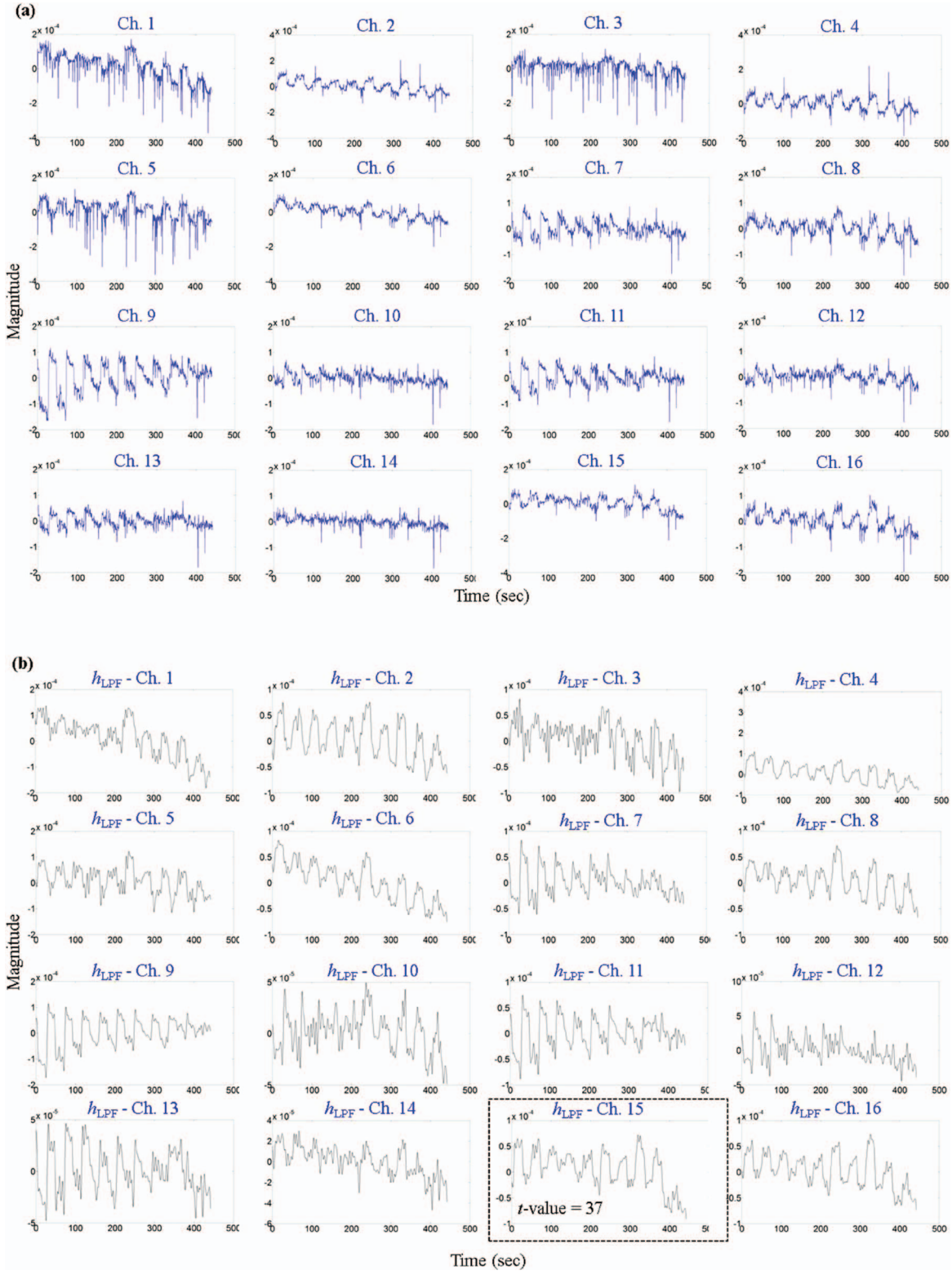

FIG. 5. Comparison of h_{LPF}'s and ICs (Subject 8): (a) NAVI HbO data, (b) low-pass-filtered (LPF) signals of (a) with cut-off frequency 0.18 Hz, and (c) the obtained 16 ICs.

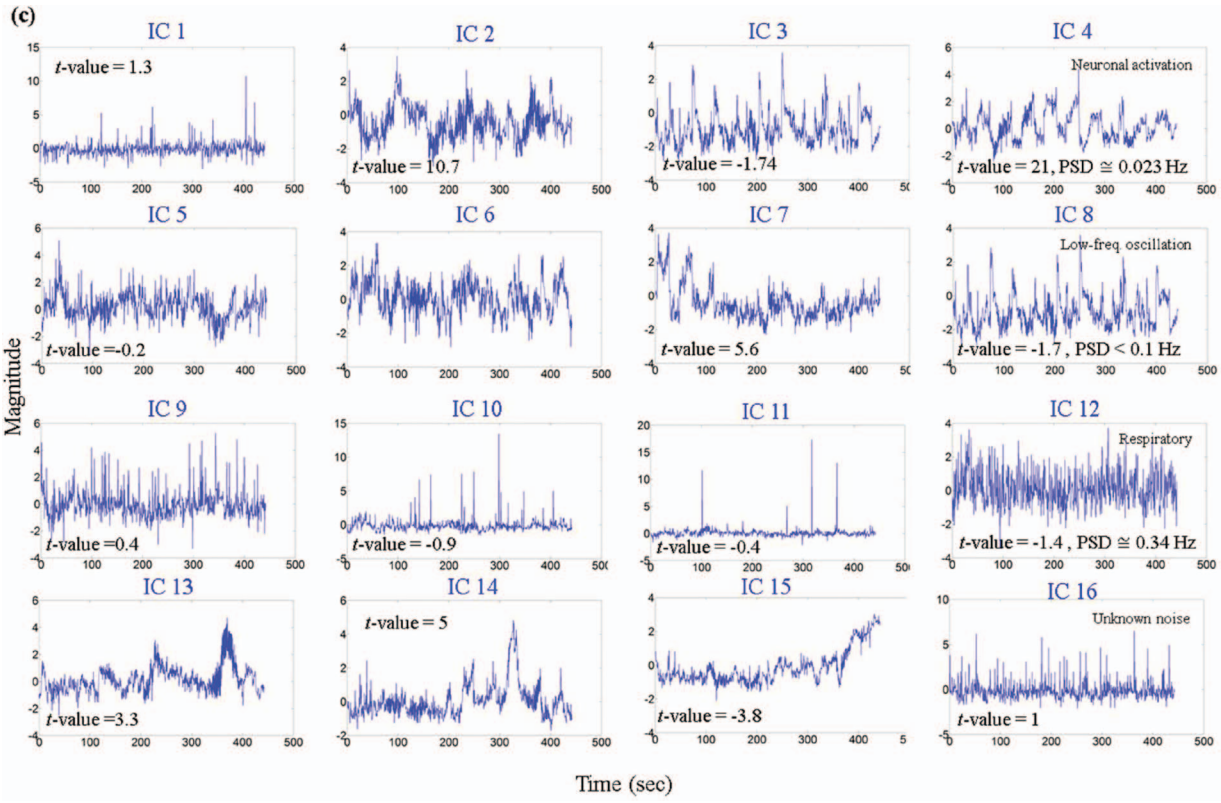

FIG. 5. (*Continued*.)

Infrared Analysis, Visualization and Imaging Suite, NIRx, USA) was used (Figure 4). Figure 5(a) shows the entire 16-channel NAVI HbO data for Subject 8. Figure 6 shows a typical example of raw HbO, HbR, and HbT (i.e., HbO + HbR) data (Subject 1, Ch. 12). The hemodynamic responses are normally affected by the subject's respiration, heartbeat, and low-frequency oscillation in the brain. These processes, in contrast to the original hemodynamic response to stimuli, are referred to as physiological noises. One way to remove such noises (e.g., respiration: ∼0.2–0.3 Hz; cardiac: ∼1 Hz) is to use a low-pass filter. In the work of Fox and Raichle,[20] for example, a low-pass filter with a cut-off frequency of 0.15 Hz was used. In the present study, similarly, the post-NAVI hemodynamic signals (i.e., Figure 5(a)) were low-pass filtered with a cut-off frequency 0.18 Hz (Figure 5(b)). The LPF signals were denoted $h_{\mathrm{LPF}}(k)$ (Figure 4).

Then, the Fast ICA v.2.5 algorithm (http://www.cis.hut.fi/projects/ica/fastica, or Ref. 1) was employed to identify 16 ICs (Figure 5(c)) from the 16-channel data (Figure 5(a)). This algorithm, notably, used a pre-processing low-pass filter with a cut-off frequency of 0.89 Hz (which is almost the Nyquist frequency of 1.81 Hz) in order to enhance the convergence speed of the processing, thereby enabling computation of the respective ICs within 600 steps. To identify the particular ICs associated with the hemodynamic responses to the arithmetic tasks, the *t*-test

$$t_j = \frac{\overline{IC_j(k)} - \overline{h_M(k)}}{\sqrt{\frac{\sigma^2_{IC_j}}{N} + \frac{\sigma^2_{h_M}}{N}}}, \tag{6}$$

for two signals was conducted, where subscript j denotes the jth IC among the 16 ICs, $\overline{IC_j(k)}$ and $\overline{h_M(k)}$ are the means of

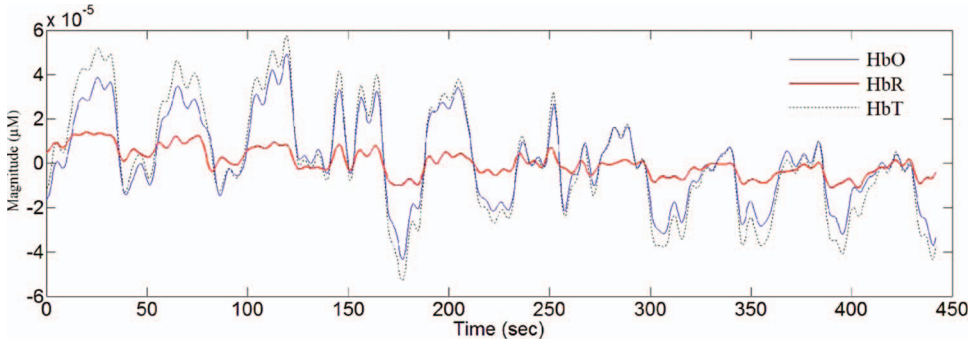

FIG. 6. A typical example of raw HbO, HbR, and HbT data (Subject 1, Ch. 12).

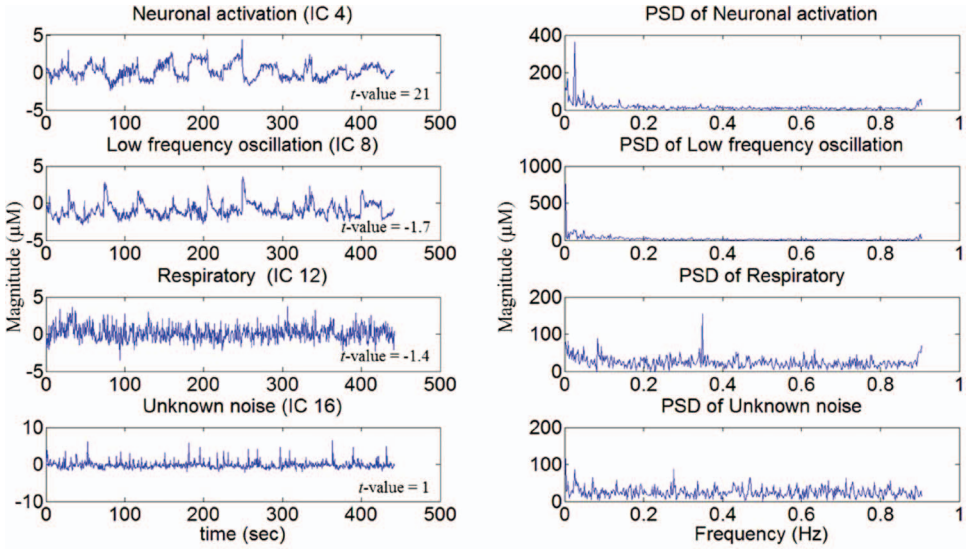

FIG. 7. PSDs of typical 4 ICs chosen from Figure 5 (Subject 8).

$IC_j(k)$ and $h_M(k)$, respectively, and σ_{IC_j} and σ_{h_M} represent the respective standard deviations. The t-values of all of the ICs are indicated in Figure 5(c). Normally, it is considered that the IC with the highest t-value is associated with the hemodynamic response to a given stimuli; however, where there are multiple ICs having similar t-values, their spectrums also should be checked. Figure 7 shows the PSDs of IC 4, IC 8, IC 12, and IC 16, respectively. As can be seen, IC 4 had the highest t-value (i.e, 21) with a PSD of around 0.023 Hz, which was near the stimulation frequency (Figure 2(b)). Thus, IC 4 was applied as the primary IC to the reconstruction of the hemodynamic response to the stimuli pattern.

Now, let the primary IC be at $j = p$. Then, the hemodynamic response to the given stimuli can be reconstructed as

$$h_{\mathrm{ICA}}(k) = IC_p(k) + \sum_{j=1, j\neq p}^{M} \frac{t_j}{\sum_{j=1}^{M} |t_j|} IC_j(k), \qquad (7)$$

where subscript p stands for the primary IC, and M is the total number of ICs.

III. RESULTS

The hemodynamic responses of the eight subjects were measured from their prefrontal cortex. The 10 arithmetic-task sessions were clearly distinguishable by visual inspection. As expected, HbO and HbT increases were manifested during the tasks (e.g., Subject 1, Ch. 12; Figure 6). This trend was apparent in some of the raw data (Figure 5(a)), but was not clear in many channels. However, it became clearer after low-pass filtering with the 0.18 Hz cut-off frequency (Figure 5(b)). The t-value of $h_{\mathrm{LPF}}(k)$ of Ch. 15 was 37, the highest.

With respect to the obtained ICs (Figure 5(c)), the following observations were made. Except IC 4, the t-value of which was 21, no clear distinctions among the task sessions was seen, owing to the fact that the other ICs were supposed to represent other phenomena. Also, in referencing the spectrums of all 16 ICs (Figure 7), IC 8 was found to be associated with low-frequency oscillation noise (<0.1 Hz), IC 12 with respiratory noise (~0.3 Hz), and IC 16 with unknown noise.

Figure 8 compares two hemodynamic responses with the modeled hemodynamic response: the thin solid line represents the hemodynamic response reconstructed using Eq. (7), and the thick dotted line is the highest t-value signal obtained by low-pass filtering with a 0.18 Hz cut-off frequency. The drifting of the signal from 360 to 450 s might have been due to incautiousness, though such noise was completely removed from $h_{\mathrm{ICA}}(k)$. It is also noteworthy that the t-value of $h_{\mathrm{ICA}}(k)$ increased to 51, whereas the highest t-value was 37. This result, especially, used in Eq. (7) increased the t-value than using only four ICs with high t-values (dotted) as shown in Figure 9.

To evaluate the overall noise-reduction effect of the ICA method in comparison with the low-pass filter approach, and to confirm the accuracy of Figure 8 results, the individual t-values for all of the eight subjects were compared (Figure 10). The post-ICA p-value averaged for all of the subjects was statistically significant ($p < 0.0005$). Across all of the subjects, ICA yielded much higher t-values. The SNR, defined as the ratio of the mean value of the signal during a task period and the standard deviation of the noise during a rest period, increased significantly for every subject. The SNR averaged over all HbO of the subjects improved from 0.66 to 4.33.

IV. DISCUSSION

The present study demonstrated the potential of our ICA method to separate physiological noises and motion artifacts from a stimuli-evoked signal and obtain the original hemodynamic response. The ICs associated with the physiological signals (i.e., low-frequency oscillation, respiration) and motion artifacts could be identified by reference to their spectral densities. Indeed, isolating the key IC(s) associated with the original hemodynamic response is essential if accuracy

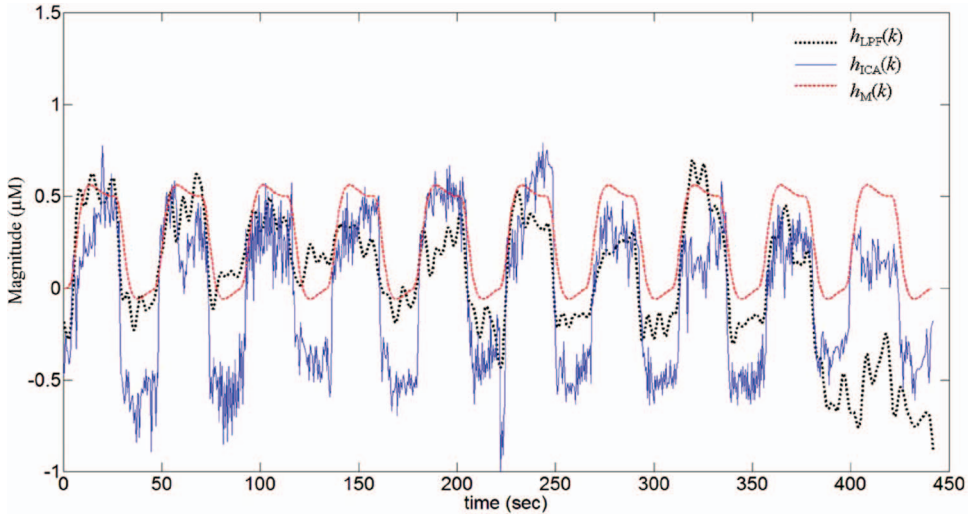

FIG. 8. HbO comparison (Subject 8): the low-pass-filtered (LPF) signal $h_{LPF}(k)$ at Ch. 15 (dotted), the reconstructed hemodynamic response $h_{ICA}(k)$ using Eq. (7) (solid), and the modeled hemodynamic signal $h_M(k)$ (the t-value between $h_{LPF}(k)$ and $h_M(k)$ is 37 and that between $h_{ICA}(k)$ and $h_M(k)$ is 51).

is to be maintained. In these ways, fNIRS in brain engineering can be facilitated and expedited using the developed method.

The steps entailed in applying the ICA method to the analysis of fNIRS signals are as follows: (i) separate signals to ICs consisting of neuronal activation, low-frequency oscillation, respiratory signal, and motion artifact noise (Figure 5(c)) in order, crucially, to obtain significant ICs while eliminating unwanted ICs; (ii) confirm their spectral densities; (iii) reconstruct the hemodynamic response by weighting the high-t-value ICs more and the low-t-value ICs less (e.g., Eq. (7)); (iv) determine whether the reconstructed hemodynamic response has an increased t-value relative to the low-pass-filtered signals (Figure 8); (v) confirm that this trend holds over all subjects.

We were able to separate physiological noises (low-frequency oscillation and respiratory signals) and an unknown noise identified as motion artifacts. Two of the ICs in Figure 7 represent the low-frequency oscillation and respiratory signals, which are clearly verifiable by their power-spectral densities. It is notable that the IC associated with the cardiac signal could not be detected, due to the fact that low-pass filtering of 0.89 cut-off frequency was applied prior to the Fast ICA. However, this low-pass filtering enhanced the Fast ICA processing. Overall, the obtained results suggest that the proposed method can effectively identify task-related brain activation in time-series while reducing noises from motion artifacts and physiological processes. The results indicate, moreover, that our ICA methodology, enabling quick construction of topographic brain-activation maps, can be

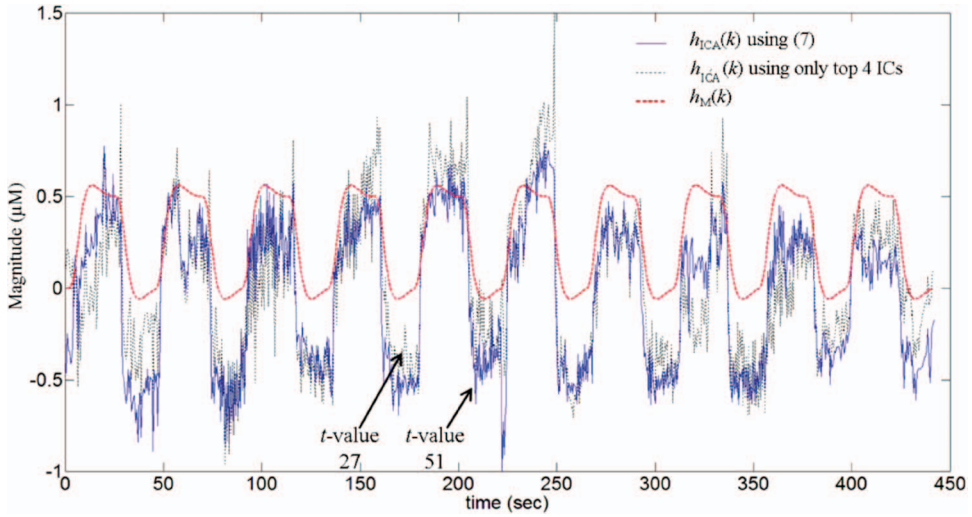

FIG. 9. Comparison of $h_{ICA}(k)$ using (7) (solid) and $h_{\acute{I}CA}(k)$ using only four ICs with high t-values (dotted): The drifting behavior of $h_{LPF}(k)$ during 360-450 s has been removed.

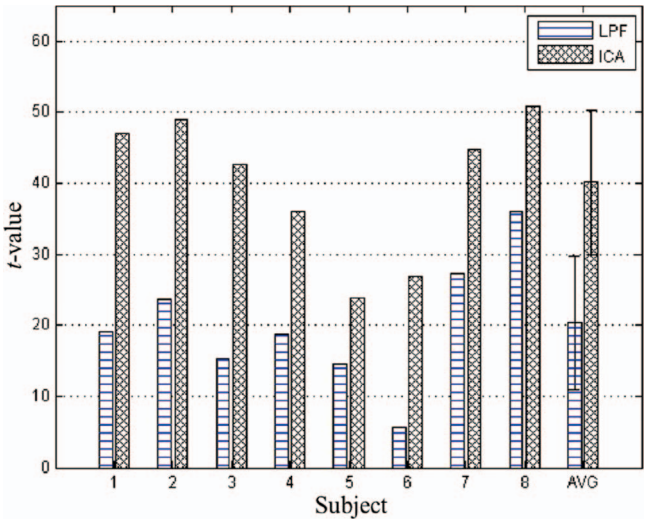

FIG. 10. Comparison of the highest t-values of $h_{\mathrm{LPF}}(k)$ and $h_{\mathrm{ICA}}(k)$, respectively, for all 8 subjects and their grand averages.

especially useful in brain-computer interfaces and many other fNIRS-based applications.

V. CONCLUSIONS

A proposed ICA method was implemented to process arithmetic-task data in the prefrontal cortex. It could effectively separate physiological noises (spontaneous fluctuation and respiratory signals) and motion artifacts for all 16 channels employed. Significant t-value increases for all eight subjects, in a comparative evaluation with conventional low-pass filtering, were observed after reconstruction of the hemodynamic response using the ICs found. In summary, the utility of the ICA method as a means of reducing noise contamination in a targeted brain area was demonstrated.

ACKNOWLEDGMENTS

This work was supported by the National Research Foundation of Korea funded by the Ministry of Education, Science, and Technology, Korea (Grant No. MEST-2012-R1A2A2A01046411).

[1]A. Hyvarinen and E. Oja, Neural Networks **13**, 411 (2000).
[2]K. Goto, Y. Hoshi, M. Sata, M. Kawahara, M. Takahashi, and H. Murohashi, J. Biomed. Opt. **16**, 127003 (2011).
[3]A. Hyvarinen, IEEE Trans. Neural Networks **10**, 626 (1999).
[4]R. Gonzales and P. Wintz, *Digital Image Processing* (Addison-Wesley, 1987).
[5]A. Turnip, K.-S. Hong, and M.-Y. Jeong, Biomed. Eng. Online **10**, 83 (2011).
[6]A. Turnip and K.-S. Hong, Int. J. Innov. Comput. Info. Control **8**, 6429 (2012).
[7]J. Virtanen, T. Noponen, and P. Merilainen, J. Biomed. Opt. **14**, 054032 (2009).
[8]T. Katura, H. Sato, Y. Fuchino, T. Yoshida, H. Atsumori, M. Kiguchi, A. Maki, M. Abe, and N. Tanaka, J. Biomed. Opt. **13**, 054008 (2008).
[9]M. J. McKeown and T. J. Sejnowski, Hum. Brain Mapp. **6**, 368 (1998).
[10]C. F. Beckmann, NeuroImage **62**, 891 (2012).
[11]C. E. Elwell, R. Springett, E. Hillman, and D. T. Delpy, Adv. Exp. Med. Biol. **471**, 57 (1999).
[12]V. Toronov, M. A. Franceschini, M. Filiaci, S. Fantini, M. Wolf, A. Michalos, and E. Gratton, Med. Phys. **27**, 801 (2000).
[13]M. A. Franceschini, D. K. Joseph, T. J. Huppert, S. G. Diamond, and D. A. Boas, J. Biomed. Opt. **11**, 054007 (2006).
[14]H. Obrig, M. Neufang, R. Wenzel, M. Kohl, J. Steinbrink, K. Einhaupl, and A. Villringer, NeuroImage **12**, 623 (2000).
[15]T. Katura, N. Tanaka, A. Obata, H. Sato, and A. Maki, NeuroImage **31**, 1592–1600 (2006).
[16]J. Lee, S. Nemati, I. Silva, B. A. Edwards, J. P. Butler, and A. Malhotra, Biomed. Eng. Online **11**, 19 (2012).
[17]X.-S. Hu, K.-S. Hong, and S. S. Ge, Neurosci. Lett. **504**, 115 (2011).
[18]F. Orihuela-Espina, D. R. Leff, D. R. C. James, A. W. Darzi, and G. Z. Yang, Phys. Med. Biol. **55**, 3701 (2010).
[19]S. S. Kannurpatti and B. B. Viswal, J. Neurosci. Methods **146**, 61 (2005).
[20]M. D. Fox and M. E. Raichle, Nat. Rev. Neurosci. **8**, 700 (2007).
[21]X.-S. Hu, K.-S. Hong, S. S. Ge, and M.-Y. Jeong, Biomed. Eng. Online **9**, 82 (2010).
[22]F. C. Robertson, T. S. Douglas, and E. M. Meintjes, IEEE Trans. Biomed. Eng. **57**, 1377 (2010).
[23]I. Schelkanova and V. Toronov, Biomed. Opt. Express **3**, 64 (2012).
[24]Y. J. Tong and B. D. Frederick, NeuroImage **61**, 1419 (2012).
[25]J. Markham, B. R. White, B. W. Zeff, and J. P. Culver, Hum. Brain Mapp. **30**, 2382 (2009).
[26]S. Patel, T. Katura, A. Maki, and I. Tachtsidis, Adv. Exp. Med. Biol. **701**, 45 (2011).
[27]M. L. Flexman, H. K. Kim, R. Stoll, M. A. Khalil, C. J. Fong, and A. H. Hielscher, Rev. Sci. Instrum. **83**, 033108 (2012).
[28]Z. X. Zhang, B. L. Sun, H. Gong, L. Zhang, J. Y. Sun, B. D. Wang, and Q. M. Luo, Rev. Sci. Instrum. **83**, 094301 (2012).
[29]X.-S. Hu, K.-S. Hong, and S. S. Ge, J. Neural Eng. **9**, 026012 (2012).
[30]X.-S. Hu, K.-S. Hong, and S. S. Ge, J. Biomed. Opt. **18**, 017003 (2013).
[31]M. Aqil, K.-S. Hong, M.-Y. Jeong, and S. S. Ge, Neurosci. Lett. **514**, 35 (2012).
[32]M. Aqil, K.-S. Hong, M.-Y. Jeong, and S. S. Ge, NeuroImage **63**, 553 (2012).
[33]J. C. Ye, S. Tak, K. E. Jang, J. Jung, and J. Jang, NeuroImage **44**, 428 (2009).
[34]C. J. Cochrane, Rev. Sci. Instrum. **83**, 105108 (2012).
[35]L. Cosentino, P. Finocchiaro, A. Pappalardo, and F. Garibaldi, Rev. Sci. Instrum. **83**, 114301 (2012).
[36]L. Cosentino, P. Finocchiaro, A. Pappalardo, and F. Garibaldi, Rev. Sci. Instrum. **83**, 084302 (2012).
[37]T. Fehr, C. Code, and M. Herrmann, Brain Res. **1172**, 93 (2007).
[38]Y. Hoshi and M. Tamura, Neurosci. Lett. **150**, 5 (1993).
[39]Y. Hoshi, H. Onoe, Y. Watanabe, J. Andersson, M. Bergstrom, A. Lilja, B. Langstrom, and M. Tamura, Neurosci. Lett. **172**, 129 (1994).
[40]M. M. Richter, K. C. Zierhut, T. Dresler, M. M. Plichta, A. C. Ehlis, K. Reiss, R. Pekrun, and A. J. Fallgatter, J. Neural Transm. **116**, 267 (2009).
[41]H. Zhang, Y. J. Zhang, C. M. Lu, S. Y. Ma, Y. F. Zang, and C. Z. Zhu, NeuroImage **51**, 1150 (2010).
[42]K. J. Friston, J. T. Ashburner, S. J. Kiebel, T. E. Nichols, and W. D. Penny, *Statistical Parametric Mapping: The Analysis of Functional Brain Images* (Academic Press, San Diego, 2008).